

Deep learning based classification of motor imagery EEG signals using an improved path finder optimization algorithm

Vishwesh Jayashekar¹, Raviraj Pandian², Rajashekar Mallajamma Basavarajegowda³

¹Associate Professor, Department of Computer Science & Engineering, GSSS Institute of Engineering and Technology for Women, Mysuru, Affiliated to VTU, Belagavi, Karnataka, India

²Professor, Department of Computer Science & Engineering, GSSS Institute of Engineering and Technology for Women, Mysuru, Affiliated to VTU, Belagavi, Karnataka, India

³Associate Professor, Department of Computer Science & Engineering, GSSS Institute of Engineering and Technology for Women, Mysuru, Affiliated to VTU, Belagavi, Karnataka, India

(Received 17 April 2024; Final version received 17 July 2024; Accepted 29 July 2024)

Abstract

Motor Imagery Brain-Computer Interfaces (MI-BCIs) are systems based on AI that collect patterns of brain activities in mental movement and translate these movements through external devices. The identification of motor intention by evaluating Electroencephalogram (EEG) signals is an important issue in applications related to Brain-Computer Interfaces (BCI). In this paper, an Improved Path Finder Optimization Algorithm (IPFOA) is proposed to improve the process of selecting features. The data is collected from the BCI competition IV 2a dataset and the stage of pre-processing takes place through sliding windows and 6th order Butterworth filter. The feature will be extracted from the pre-processed data using the hybrid Convolutional Neural Network (CNN) and Common Spatial Pattern (CSP) method. After this stage, the required features are selected from the extracted features using the proposed IPFOA algorithm. Finally, the classification of EEG signals takes place using a Stacked autoencoder, a classifier based on a Deep Neural Network. The experimental results show that the proposed approach achieved a better accuracy of 98.40% which is comparatively higher than the existing approaches.

Keywords: Brain Computer Interface, Convolutional Neural Networks, Deep Learning, Electroencephalogram, Motor Imagery, Path Finder Optimization.

1. Introduction

A control system known as a brain-computer interface (BCI) facilitates communication between the brain and other devices by using signals produced by brain activity Electroencephalogram (EEG) vibrations created by the brain's response are typically computed based on cerebral actions (Xiao X et al. 2021 & Yu X et al. 2021). The vibrations are in the pattern of bioelectric signals which are easy to operate and safe. The system produces direct communication between the brain and the machine without any intermediates; it is also considered as a modern and extraordinary interaction method between computers and humans (Meng X et al. 2021 & Mahapatra et al. 2022).

A technology called the Motor Imagery Brain-Computer Interface (MI-BCI) modifies how the brain reacts to physical actions. EEG is used by systems based on MI-BCI to track every mental activity. Additionally, MI-BCI has the ability to accurately identify concepts of physical activities including the movement of the hands,

legs, and feet, among others (Tibrewal et al. 2022). The applications of EEG are widely utilized for the applications of BCI because of its high temporal resolutions and simple implementation. The BCI system helps in recording the activities of the brain and processes it to an artificial limb or wheelchair. The applications of BCI play a major role in psychology, entertainment purposes, gaming, smart buildings, neuromarketing, etc. (Idowu et al. 2021 & Cherloo et al. 2021).

There are many conventional Machine Learning (ML) algorithms such as random forest, decision tree, support vector machine etc., employed in the classification of motor imagery of EEG (Yang et al. 2021). The conventional ML algorithms in MI-BCI are based on handcrafted features (Musallamet al. 2021), and the features are extracted using a general method such as Common Spatial Pattern (CSP). Generally, employing CSP on the time series of EEG consists of a bandpass filter with a wide range of frequencies (for example, 5-45 Hz) (Malan et al. 2021). The CSP approach extracts the multi-channel EEG signals for classifying the signals on



Fig 1. EEG signal classification using IPFOA

the right and left hands. Moreover, the CSP extracts feature spatially from each sub-band. For large amounts of sub-bands, an autoencoder (AE) is utilized to lessen the dimensionality of more sub-band features in CSP (Tang et al. 2021). However, there are certain limitations in CSP such as the sensitivity of noise and the issue of overfitting (Darvish et al. 2021 & Keerthi et al. 2021), which are overcome in the proposed method. Additionally, employing CSP in the field of ML to obtain accurate results remains as a challenging task (Mirzaei et al. 2021). So, Deep Learning methods (DL) are considered state-of-the-art in various fields such as recognition of speech, natural language processing, and so on. Since the DL method has developed a graphic processing unit, it attributes high-level feature extraction and classification methods (Phadikar et al. 2023). This reason made researchers and scholars initiate the MI-BCI-based classification of EEG signals. DL consists of a Deep Neural Network (DNN) that is broadly utilized in the field of recognition of MI using EEG signals (Hermosilla et al. 2021).

The motor imagery signals consist of undesired noises and blurred signals which diminish the accuracy of the classification model (Dagdevir et al. 2023). This research undertakes the aforementioned issues which rely on the existing algorithms as motivation, and focuses on developing a DNN classifier that efficiently classifies the EEG signals based on MI-BCI.

The main contributions of the paper are highlighted below:

The proposed IPFOA achieved better performance in selecting the features from the sensorimotor rhythms to classify the EEG signals.

The CNN-based CSP is utilized in extracting the desired features according to the needs of the user.

From various optimization methods, the proposed IPFOA achieved the highest metrics during evaluation and attained comparatively better results than the existing methods.

The remaining paper is organized as follows; the proposed method is discussed in Section 2. The results

and discussion are provided in Section 3, and the conclusion of this research is presented in Section 4.

2. Proposed Method

The EEG classification involves four steps namely, pre-processing or artifacts removal using the 6th order Butterworth filter following the feature extraction using the hybrid CNN and CSP methods and later feature selection using the proposed method, and finally classification using the stacked autoencoder. It is represented in the **Figure 1**.

2.1 Dataset

This paper is based on the information obtained from the BCI Competition IV 2a dataset. The dataset is introduced by the Graz University, Austria, which is utilized to compute the efficiency of the motor imagery EEG encoding method (Ang et al. 2012). The collection of the dataset includes EEG data from nine healthy people who perform four different motor imagery tasks, including moving the tongue, both feet, both hands, and both right and left hands, and 22 EEG electrodes are used to record the data at a sample rate of 250 Hz. The signals are band-pass filtered between 0.5 Hz and 100 Hz, and notch filtered at 50 Hz. For each subject, 2 periods on various days are verified, with 288 trials in each session. Each trial has a sampling interval of 3s, yielding 750 sample points overall. Each trial is used as a sample in this research and is considered in a 2D matrix measuring 22 by 750. The 750 columns of a sample correspond to the EEG data from the 750 sample points, and 22 rows of a sample correspond to the recorded signal from 22 electrodes. The original input signal is represented in **Figure 2** and the input signal obtained from one electrode is represented in **Figure 3**. The EEG signal of the person's left hand (**Figure 4**), right hand (**Figure 5**), foot and tongue are represented.

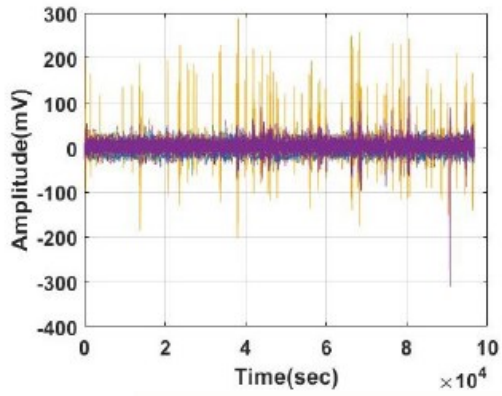


Fig 2. Input Signal

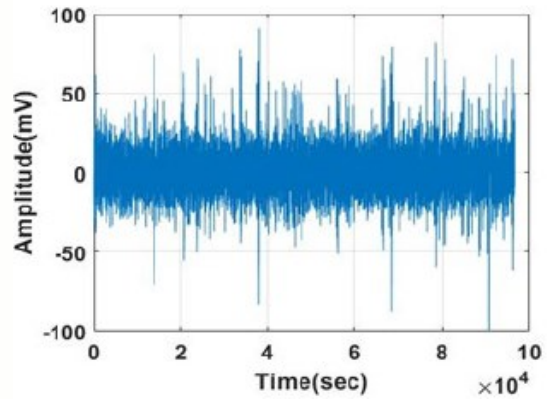


Fig 3. Input Signal for 1-Electrode

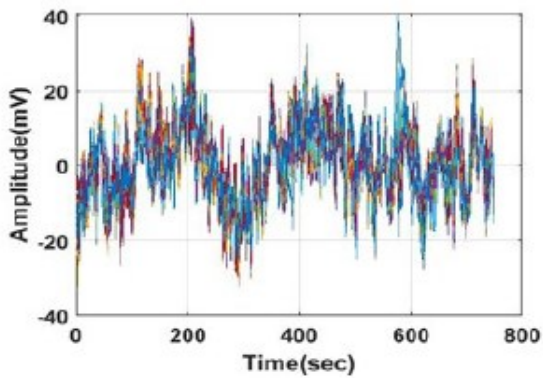


Fig 4. Class-1 for all Electrodes (Left hand)

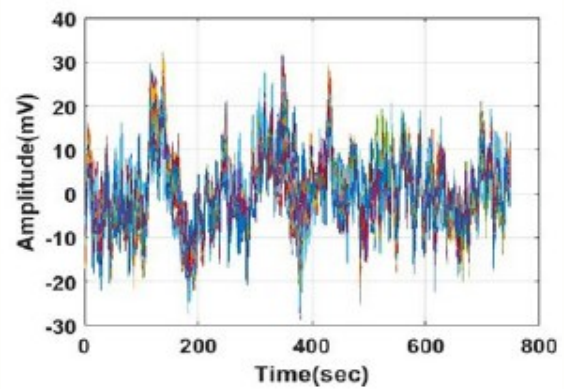


Fig 5. Class-2 for all Electrodes (Right hand)

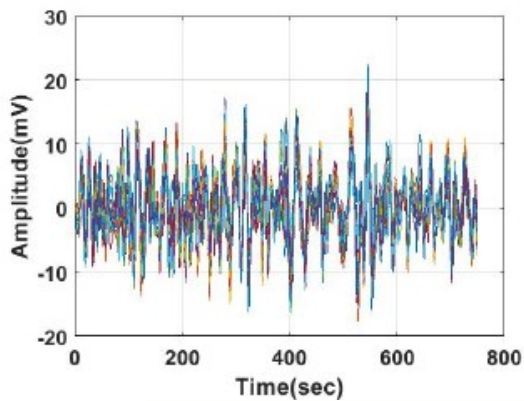


Fig 6. Pre-processing Class-1 (Left hand)

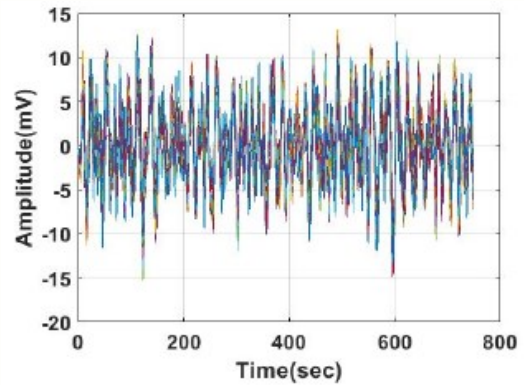


Fig 7. Pre-processing Class-2 (Right hand)

2.2 Pre-Processing

In the stage of pre-processing, the sliding window is used based on the Longest Consecutive Repetition (LCR). LCR (Gaur et al. 2021 & Saideepthi et al. 2023) is known as the longest repeating sequence of an element, for instance, in 5655566, '555' is considered the longest repeating sequence. Here, a total of 5 overlapping windows are used which are represented as $TT1$ to $TT5$. The first window starts ($TT1$) from the time period of 1.0 s, the second window ($TT2$) starts from 1.1 to 2.1, and the final window ($TT5$) starts from 4.4 to 5.5. The data is band-passed using the butterworth filter of order 6 and the signals of EEG occur in the rhythms of μ and β . The rhythms of μ and β are attained from the signal of EEG to indicate the information regarding motor imagery. The equation of the Butterworth filter is represented in Eq. (1). The pre-processed signals of the left hand and right hand are represented in **Figures 6** and **7**, respectively.

$$H(z) = \frac{B(z)}{A(z)} \quad (1)$$

$$= \frac{b(1) + b(2)z^{-1} + \dots + b(n+1)z^{-n}}{a(1) + a(2)z^{-1} + \dots + a(n+1)z^{-n}}$$

2.3 Feature Extraction

In this paper, the extraction of features takes place using a Convolutional Neural Network (CNN) and Common Spatial Pattern (CSP) (Rusnac et al. 2022, Rusnac et al. 2022, Sun et al. 2022 & Jin et al. 2021). The first layer in the CNN designs is an input layer, while the subsequent layers are made up of convolutional, max-pooling, and/or average pooling layers. To prevent overfitting, dropout layers are included in between the several convolutional layers. A thick layer, a fully linked layer and a soft maximum layer make up the final classification layer. The deeper layers of CNN are created to learn higher-level features by breaking down the input into complex structures, whereas the first layer of CNN learns fundamental features through filtering. The learned features from the previous layers are combined in the final, fully linked layer for classification. CNN uses backward propagation methods to reduce error, and forward propagation algorithms to discover the output.

The major goal of CSP is to investigate the spatial filters that reduce the variance of class and help in band pass filtering the multichannel signals of EEG. The method based on CSP attains optimum

discrimination for the tasks based on MI-BCI on band power features. The optimized function of the CSP method using spatial filter $P(x)$ is represented in Eq. (2).

$$P(x) = \frac{x^T p_1^T p_1 x}{x^T p_2^T p_2 x} = \frac{x^T c_1 x}{x^T c_2 x} \quad (2)$$

Where the transpose of the matrix is represented as T , the training data of the matrix is represented as P_i where the rows are considered spatial points and the channels are represented as Columns. For the particular class i , the spatial covariance matrix is represented as C_i . There are many ways to solve the problems in optimization, here the technique is based on visualizing the function $P(x)$ when the rescaling occurs in the filter x . The $P(kx) = P(x)$, where k is denoted as a constant value of rescaling the filter. So, minimizing $P(x)$ is similar with $x^T c_1 x$ to the constraint $x^T c_2 x = 1$. The constrained optimization function using the method of Lagrange multiplier is represented in Eq. (3),

$$L(\beta, x) = x^T C_1 x - \beta(x^T C_2 x - 1) \quad (3)$$

Where the Lagrange multiplier is denoted as β , a derivative of L concerning x is denoted as 0. The filter x minimizing L is denoted using the Eq. (4),

$$\frac{\partial L}{\partial x} = 2x^T C_1 x - 2\beta x^T C_2 x = 0 \quad (4)$$

Where ∂ is the derivative related to the Lagrange multiplier. From this, the value of β is attained as $C_2^{-1} C_1 x$, so the value of the Eigenvector is represented in Eq. (5),

$$z = C_2^{-1} C_1 x \quad (5)$$

Where, z is the feature of CSP which is attained by linearly transforming the signals of EEG.

2.4 Feature Selection

The PFOA (Halder et al. 2022) is a swarm-intelligence-based meta-heuristic technique which was introduced in 2019. The PFA's computing process was motivated by the collective behaviour of any animal group in search of food. The animal population is divided into two groups, the leader and the followers, which imitates the leadership position and the followers to mathematically describe the algorithm. To find the ideal food zone, the leader is responsible for discovering new areas in the search area. The leader also leaves a footprint that aids the follower's upcoming

reorientation, and helps followers to find the path by following the footsteps. According to footsteps and perception, the followers follow the pathfinder. In the optimization of PFA, the part of followers and the leaders do not remain constant, it varies according to the search capability of individuals. So, the pathfinder may be a follower or leader. In the process of searching, the process of PFOA takes place in two stages. The first stage is the pathfinder phase, where the pathfinder is represented as $XXPP$ and it is represented in Eq. (6),

$$X_p^{k+1} = X_p^k + 2 \times r_3 \times (X_p^k - X_p^{k-1}) + A, \quad (6)$$

$$\vec{r}_3 \in \{R \text{ and } (1, D)\}$$

Where, t represents the iteration counter and the dimensional vector set D of the random numbers which are created uniformly within the range $[0,1]$, and signified as $\{R \text{ and } (1,D)\}$. The A is denoted as a parameter at each iteration and is represented in Eq. (7),

$$A = u_2 \times \exp\left(\frac{-2k}{kmax}\right), \vec{u}_2 \in \{R \text{ and } (1, D)\} \quad (7)$$

Where the maximum number of iterations is represented as $kmax$.

In the second stage, every individual follower ii varies its position which is represented in Eq. (8) as follows,

$$X_1^{k+1} = X_1^k + 2 \times R_1 \times (X_j^k - X_1^k) + R_2 \times (X_p^k - X_1^k) + \varepsilon, i \geq 2 \quad (8)$$

$$\varepsilon = \left(1 - \frac{k}{kmax}\right) \times u_1 \times Dist_{i,j}, \vec{u}_1 \in \{R \text{ and } (1, D)\} \text{ and } Dist_{i,j} = \|X_1^k - X_j^k\| \quad (9)$$

In Eq. (9), X_j^k represents the adjacent individual of the i^{th} follower and $R_1 = \alpha.r_1$, $R_2 = \alpha.r_2$. where \vec{r}_1 and $\vec{r}_2 \in \{R \text{ and } (1,D)\}$. The coefficient of interface with a neighbor is denoted as α and the coefficient of attraction in a random distance is denoted as β . The value of ε is computed using the formula given in Eq. (9). To perform a multi-dimensional search, the values of A and ε must be limited to a specific range.

2.5 Improved Path Finder Optimization Algorithm (IPFOA)

The IPFOA is obtained by extending three features in existing PFA, the addition of features includes, (i) adding the mechanism of the wizard in PFA, (ii) adding the operators, (iii) improving the mechanism of mutation to branch out the individuals and increase the ability of algorithms. The following sections briefly explain the modifications to PFA.

2.5.1 Adding the mechanism of the wizard in PFA

In this stage, the pathfinder is considered a guide where the guide can be replaced using the iteration of the algorithm. During every iteration, the individual who has a small fitness value in the group is considered a guide. The guide provides useful information from the obtained experience to the followers. It is represented in Eq. (10).

$$X_1^{new} = X_1^{old} + rand. (X_1^{guide} - TF \times Mean) \quad (10)$$

In Eq. (10), X_1^{new} gets updated using X_1^{old} and the best individual in the group is represented as X_1^{guide} . The mean value of the follower present in the iteration is represented as $Mean$ and the random value that lies between the range $[0,1]$ is represented as $rand$. The passing weight is denoted as TF , where $TF = \text{round}[1 + \text{rand}(0,1)\{2-1\}]$. When the fitness value of X_1^{new} has better value than X_1^{old} , then X_1^{old} is replaced with X_1^{new} . The guide offers better solutions for all the people and helps improve the speed during converging.

2.5.2 Adding the Operators

In this stage, the stage of the follower is improved and the addition of two operators takes place to regulate the search direction. Here, the value of accept operator P is 0.8 and $etac$ is 20, and the values of P and $etac$ are determined from numerous experiments. When the value of P is greater than the provided random value, the position of the follower is organized consequently using the Eq. (11). In contrast, the addition of an exchange operator takes place and the position of the follower is organized using the Eq. (11-13).

$$X_1^{k+1} = X_1^k + 2(rand - 0.5) \times (X_1^{guide} - X_1^k) \quad (11)$$

$$X_1^{k+1} = X_1^k + \gamma \times R_1 \times (X_j^k - X_1^k) + \gamma \times R_2 \times (X_p^k - X_1^k) + \varepsilon, i \geq 2 \quad (12)$$

$$\beta = \begin{cases} \frac{1}{2r\text{etac}+1r} \leq 0.5 \\ \frac{1}{2(1-r)} \quad \text{else} \end{cases} \quad (13)$$

Where the number of iterations are represented as k and X_1^{k+1} is upgraded as X_1^k . The best individual in the iteration is represented as X_1^{guide} and the random value lies between the range $[0,1]$, represented as $rand$. $R1$ and $R2$ are denoted as random variables in the range of $[0,1]$. The neighboring individual is represented as X_j^k and the interaction degree with neighboring individuals or leaders is represented as γ , which is determined by random variables r and $etac$. The best individual initiates its direction by learning and communicating with the leader and the neighboring individuals. This stage helps in increasing the mining capability of the algorithm.

2.5.3 Mechanism of Mutation

The mutation stage is employed in the search phase to maintain equilibrium between exploration and exploitation. The process of mutation is used to create a new population with fewer individual differences. People who are aware of their surroundings do searches at random inside the designated search zone, while others who appear to be less capable do not perform searches. To offer individuals an opportunity to increase the diversity of the population and keep the algorithm from reaching local optimality, the mutation mechanism is implemented. The introduction of the mutation process increases population diversity, gives an opportunity for novices to learn from more seasoned individuals, and keeps the algorithm from reaching local optimality. It uses a specific proportion of the information from multiple individuals as the amount of individual disturbance. The mutation probability ensures that the majority of people have the chance to learn (pcR). If the value of pcR is smaller than 0.5, it will be harder for weaker people to learn because the experimental effect won't be as noticeable. When the value of $pcRis$ greater than 0.8, the mutation takes

place among all individuals in the group, so the value of $pcRis$ allotted between 0.5 and 0.8. The mathematical representation of the mutation mechanism is represented in Eq. (14),

$$X_1^{k+1} = X_m^k + pcR.(X_n^k - X_1^k) \quad (14)$$

Where m and n denotes the mutation which takes place in m th individual and n th individual of the population respectively.

2.6 Classification

In this stage, the classification of EEG signals takes place using Stacked Autoencoder (SAE) (Vafaei et al. 2023 & Li Q et al. 2022). An autoencoder (AE) is a network that consists of one input, hidden and output layer. The total neurons present in the output layer equals the total neurons in the layer of input. At the time of training, the input xx is mapped with the hidden layer to give yy as provided in Eq. (15), as a hidden output. Afterward, yy gets mapped with the layer at the output to provide the value of z (provided in Eq. (16)). The mentioned steps are represented as,

$$y = f(W_y x + b_y) \quad (15)$$

$$z = f(W_z y + b_z) \quad (16)$$

Where f is known as a function of activation and is represented in Eq. (17),

$$f(a) = 1/(1 + \exp(-a)) \quad (17)$$

Wz and Wy are known as the weight from the layers of output and weights from the layer of input to the hidden layer respectively. The bias values of hidden and output layers are represented as b_y and b_z respectively. When the value of W_y is fixed as W_z , the weights are tied and this helps in obtaining the parameters of the model by reducing the cost function, which is represented in Eq. (18),

$$\arg \min_{W, b_y, b_z} [E(x, z)] \quad (18)$$

The reconstruction error is represented as $E(x, z)$, when the network is trained to reconstruct the values of output to the values of input. The model parameters can be reorganized by the Eq. (19-21),

$$W = W - \eta \frac{\delta E(x, z)}{\delta W} \quad (19)$$

$$b_y = b_y - \eta \frac{\delta E(x, z)}{\delta b_y} \quad (20)$$

$$b_z = b_z - \eta \frac{\delta E(x, z)}{\delta b_z} \quad (21)$$

The learning rate of the algorithm is denoted as η . After the training of AE, the features in the hidden layers are utilized for classification in the layer of the deep network of AE, which is referred to as a Stacked Auto Encoder (SAE). The SAE is composed of layers of input and output along with numerous AEs. Every individual layer of the AE (Zeng et al. 2023 & Wang et al. 2022) is trained separately and the output of the hidden layer in AE is utilized as input for the next layer in a deep neural network.

3. Result and Discussion

The results and discussion of the IPFOA are explained in this section. The design and implementation of the DL model using IPFOA are done by MATLAB R2020b version 9.9. The system utilized in classification involves specifications of an i5 processor with 6GB RAM. The major part of IPFOA is to attain precise and accurate classification of EEG motor imagery signals.

3.1 Performance Analysis

The performance of the classifier with feature selection in DNN is compared with the existing Multiclass Support Vector Machine (MSVM), K-Nearest Neighbor (KNN), Random Forest (RF), Decision Tree (DT), Neural Network (NN) and Deep Neural Network (DNN). The results are validated with 5-fold cross-validation with 20% testing and 80% training. The performance analysis of the classifier with feature selection is represented in **Table 1**.

Table 1. Performance Analysis of Various Classifiers with Feature Selection

Classifier	Acc* (%)	Sen* (%)	Spe* (%)	F1* (%)	Pre* (%)
MSVM	94.23	92.79	96.91	94.93	97.17
KNN	95.28	91.96	93.79	92.82	93.71
RF	95.55	96.49	93.96	95.24	94.03
DT	96.96	92.80	95.74	92.03	91.28
NN	96.96	94.14	93.39	94.09	94.05
DNN	98.40	99.00	98.91	99.46	99.92

Acc:* Accuracy, *Sen*:* Sensitivity, *Spe*:* Specificity, *F1*:* F1-score, *Pre*:* Precision

Table 2. Performance Analysis of Various Classifiers without Feature Selection

Classifier	Acc* (%)	Sen* (%)	Spe* (%)	F1* (%)	Pre* (%)
MSVM	90.87	89.14	88.60	91.09	87.61
KNN	92.69	91.77	93.71	91.26	90.75
RF	90.32	88.80	89.75	90.01	91.26
DT	93.95	92.19	90.28	91.85	91.51
NN	94.03	90.49	93.68	91.09	91.70
DNN	95.44	93.45	94.66	93.67	93.89

Acc:* Accuracy, *Sen*:* Sensitivity, *Spe*:* Specificity, *F1*:* F1-score, *Pre*:* Precision

From **Table 1** and **Table 2**, it is concluded that the performance of the Stacked Auto-Encoder (SAE), a DNN classifier provides better results in accuracy (95.44%), sensitivity (93.45%), specificity (94.66%), F1 score (93.67%), and precision (93.89%). **Table 3** represents the performance of the optimization algorithms such as Particle Swarm Optimization (PSO), Ant Colony Optimization (ACO), Fruit fly Optimization algorithm (FOA), Path Finder Optimization (PFOA), and the proposed IPFOA. From the results of **Table 3**, it is concluded that the proposed IPFOA has the highest evaluation metrics when compared with other optimization algorithms for feature selection

Table 3. Evaluation of Optimization Algorithms

Algorithms	Acc* (%)	Sen* (%)	Spe* (%)	F1* (%)	Pre* (%)
PSO	87.66	90.27	89.93	90.49	90.72
ACO	92.35	91.70	90.99	91.34	90.99
FOA	94.78	93.36	92.16	93.73	94.10
PFOA	94.96	94.25	93.25	94.91	95.57
Proposed (IPFOA)	98.40	99.00	98.91	99.46	99.92

Acc:* Accuracy, *Sen*:* Sensitivity, *Spe*:* Specificity, *F1*:* F1-score, *Pre*:* Precision

3.2 Comparative Analysis

The comparative analysis of the method used for feature extraction of the hybrid (combination of CNN-CSP) with the existing research is provided in this section. The existing t-distributed Stochastic Neighbor Embedding (t-SNE) and MFTL-LDA are compared to calculate the performance of the hybrid method. The hybrid method is utilized in extracting the features from the raw data which can reduce the redundancy of data and increase the speed of learning. The comparative analysis of the hybrid feature extraction method is provided in **Table 4**.

Table 4. Comparative Table

Methods	Acc* (%)	Sen* (%)	Spe* (%)	F1* (%)	Pre* (%)
t-distributed Stochastic Neighbor Embedding (t-SNE) (Song et al. 2021)	91.67	71.67	95	78.33	61.67
MFTL-LDA (Liang et al. 2020)	88.50	83.50	86	83	68.55
IDEOA (Vishwesh et al. 2023)	97.34	NA	98.01	98.72	98.54
Hybrid (proposed)	98.40	99.00	98.91	99.46	99.92

Acc*: Accuracy, Sen*: Sensitivity, Spe*: Specificity, F1*: F1-score, Pre*: Precision

3.3 Practical Applications and Implications of the Proposed Method

Using the Improved Path Finder Optimisation (IPFO) technique, BCI (Brain-Computer Interface) systems can be greatly improved. Mainly it can be used in medical rehabilitation as stroke recovery where BCIs can be used to interpret neural signals and control robotic arms, stroke patients can benefit from assistance in relearning motor abilities. To improve these systems' precision and responsiveness, IPFO can optimize signal processing. By using IPFO to increase the speed and accuracy of communication devices, BCIs can help people with severe speech or movement disabilities communicate more effectively. By optimizing the path finding in brain signal interpretation, IPFOA can greatly increase the signal-to-noise ratio in BCIs, resulting in more precise and dependable BCIs.

4. Conclusion

In this paper, the improved pathfinder optimization algorithm is proposed to efficiently classify the motor imagery EEG signals into four classes Left hand, right hand, feet, and tongue. The classification of EEG signals is performed using a DNN classifier called a stacked autoencoder. Here, the DL model is utilized to classify the Electroencephalogram (EEG) signals because they offer a method for the automatic extraction of spatiotemporal information from the signals. The features are extracted using the CNN-based CSP which efficiently extracts the features from the raw data which can reduce the redundancy of data. The extracted features undergo the process of feature selection using

IPFOA. The proposed IPFOA performs better than previous methods, according to experimental findings when the data quantity from the subject is very small. It performs better than the older techniques even if the new training data is adequate. The IPFOA offers a new concept for regulating the features of EEG in the classification task of motor imagery signals. In the future, the proposed algorithm will be applied to the real-time applications of BCI.

ACKNOWLEDGEMENTS

The paper background work, conceptualization, methodology, dataset collection, implementation, result analysis, and comparison, preparing and editing a draft, visualization have been done by first. The supervision, review of work, and project administration have been done by the second author.

REFERENCES

- Ang KK, Chin ZY, Wang C, Guan C, Zhang H. (2012). Filter bank common spatial pattern algorithm on BCI competition IV datasets 2a and 2b. *Frontiers in Neuroscience*. 2012; 6:39. <https://doi.org/10.3389/fnins.2012.00039>.
- Cherloo MN, Amiri HK, Daliri MR. (2021). Ensemble Regularized Common Spatio-Spectral Pattern (ensemble RCSSP) model for motor imagery-based EEG signal classification. *Computers in Biology and Medicine*. 2021; 135:104546. DOI: 10.1016/j.compbiomed.2021.104546.
- Darvish ghanbar K, Rezaei TY, Farzamnia, A, Saad I. (2021). Correlation-based common spatial pattern (CCSP): A novel extension of CSP for classification of motor imagery signal. *Plos one*. 2021; 16(3):e0248511. <https://doi.org/10.1371/journal.pone.0248511>.
- Dagdevir E, Tokmakci M. (2023) Determination of effective signal processing stages for brain computer interfaceon BCI competition IV data set 2b: a review study. *IETE Journal of Research*. 2023; 69(6):3144-55. DOI: 10.17485/IJST/v16i6.2076.
- Gaur P, Gupta H, Chowdhury A, McCreadie K, Pachori RB, Wang H. (2021). A sliding window common spatial pattern for enhancing motor imagery classification in EEG-BCI. *IEEE Transactions on Instrumentation and Measurement*. 2021; 70:4002709. DOI:10.1109/TIM.2021.3051996.

- Halder S, Dora BK, Bhat S. (2022). An Enhanced Pathfinder Algorithm based MCSA for rotor break-age detection of induction motor. *Journal of Computational Science*. 2022; 64:101870. DOI:10.1016/j.jocs.2022.101870.
- Hermosilla DM, Codorniu RT, Baracaldo RL, Zamora RS, Rodriguez DD, Albuerne YL, Álvarez JRN. (2021). Shallow convolutional network excel for classifying motor imagery EEG in BCI applications. *IEEE Access*. 2021; 9:98275-86. DOI:10.1109/ACCESS.2021.3091399.
- Idowu OP, Adelopo O, Ilesanmi AE, Li X, Samuel OW, Fang P, Li G. (2021). Neuro-evolutionary approach for optimal selection of EEG channels in motor imagery based BCI application. *Biomedical Signal Processing and Control*. 2021; 68:102621. <https://doi.org/10.1016/j.bspc.2021.102621>.
- Jin J, Xiao R, Daly I, Miao Y, Wang X, Cichocki A. (2020). Internal feature selection method of CSP based on L1-norm and Dempster–Shafer theory. *IEEE transactions on neural networks and learning systems*. 2021; 32(11):4814-25. DOI: 10.1109/TNNLS. 2020.3015505.
- Keerthi KK, Soman KP. (2021). CNN based classification of motor imaginary using variational mode decomposed EEG-spectrum image. *Biomedical Engineering Letters*. 2021; 11(3):235-47. DOI: 10.1007/s13534-021-00190-z.
- Liang Y, Ma Y. (2020). Calibrating EEG features in motor imagery classification tasks with a small amount of current data using multisource fusion transfer learning. *Biomedical Signal Processing and Control*. 2020; 62:102101.
- Li Q, Liu Y, Shang Y, Zhang Q, Yan F. (2022). Deep sparse autoencoder and recursive neural network for EEG emotion recognition. *Entropy*. 2022; 24(9):1187. <https://doi.org/10.3390/e24091187>.
- Meng X, Qiu S, Wan S, Cheng K, Cui, L. (2021). A motor imagery EEG signal classification algorithm based on recurrence plot convolution neural network. *Pattern Recognition Letters*. 2021; 146:134-41. DOI: 10.1016/j.patrec.2021.03.023.
- Mahapatra AK, Panda N, Pattanayak BK. (2022). An Improved Pathfinder Algorithm (ASDR-PFA) based on Adaptation of Search Dimensional Ratio for solving constrained optimization problems and optimal Feature Selection. 2022. DOI:10.21203/rs.3.rs-2115041/v1.
- Musallam YK, AlFassam NI, Ghulam M, Amin SU, Alsulaiman M, Abdul W, Altaheri H, Bencherif MA, Algabri M. (2021). Electroencephalography-based motor imagery classification using temporal convolutional network fusion. *Biomedical Signal Processing and Control*. 2021; 69:102826. <https://doi.org/10.3390/bioengineering9070323>.
- Malan NS, Sharma S. (2021). Time window and frequency band optimization using regularized neighbourhood component analysis for Multi-View Motor Imagery EEG classification. *Biomedical Signal Processing and Control*. 2021; 67:102550. DOI:10.1016/j.bspc.2021.102550.
- Mirzaei S, Ghasemi P. (2021). EEG motor imagery classification using dynamic connectivity patterns and convolutional autoencoder. *Biomedical Signal Processing and Control*. 2021; 68:102584. <https://doi.org/10.1016/j.bspc.2021.102584>.
- Phadikar S, Sinha N, Ghosh R. (2023). Unsupervised feature extraction with autoencoders for EEG based multiclass motor imagery BCI. *Expert Systems with Applications*. 2023; 213A:118901. <https://doi.org/10.1016/j.eswa.2022.118901>.
- Rusnac AL, Grigore O. (2022). CNN architectures and feature extraction methods for EEG imaginary speech recognition. *Sensors*. 2022; 22(13):4679. <https://doi.org/10.3390/s22134679>.
- Rusnac AL, Grigore O. (2022). Imaginary Speech Recognition Using a Convolutional Network with Long-Short Memory. *Applied Sciences*. 2022; 12(22):11873. <https://doi.org/10.3390/app122211873>.
- Saideepthi P, Chowdhury A, Gaur P, Pachori RB. (2023). Sliding Window along with EEGNet based Prediction of EEG Motor Imagery. *IEEE Sensors Journal*. 2023; 23(15):17703-17713. <https://dx.doi.org/10.1109/JSEN.2023.3270281>.
- Sun J, Wei M, Luo N, Li Z, Wang H. (2022). Euler common spatial patterns for EEG classification. *Medical & Biological Engineering & Computing*. 2022; 60(3):753-67. DOI: 10.1007/s11517-021-02488-7.
- Song Y, Jia X, Yang L, Xie L. (2021). Transformer-based spatial-temporal feature learning for EEG decoding. *arXiv preprint arXiv:2106.11170*. 2021.

Tibrewal N, Leeuwis N, Alimardani M. (2022). Classification of motor imagery EEG using deep learning increases performance in inefficient BCI users. *Plos one*. 2022; 17(7):e0268880. <https://doi.org/10.1371/journal.pone.0268880>.

Tang R, Li Z, Xie X. (2021). Motor imagery EEG signal classification using upper triangle filter bank auto-encode method. *Biomedical Signal Processing and Control*. 2021; 68:102608. DOI:10.1016/j.bspc.2021.102608.

Vafaei E, Rahatabad FN, Setarehdan SK, Azadfallah P. (2023). Extracting a Novel Emotional EEG Topographic Map Based on a Stacked Autoencoder Network. *Journal of Healthcare Engineering*. 2023; 2023:9223599. <https://doi.org/10.1155/2023/9223599>.

Vishwesh J, Raviraj P. (2023). Improved Differential Evolution with Stacked Auto Encoder for EEG Motor Imagery Classification. *Indian Journal of Science and Technology*. 2023; 16(6):391-400. DOI: 10.17485/IJST/v16i6.2076.

Wang Y, Qiu S, Li D, Du, C., Lu, B.L., He, H. (2022). Multi-modal domain adaptation variational autoencoder for eeg-based emotion recognition. *IEEE/CAA Journal of Automatica Sinica*. 2022; 9(9):1612-26. DOI: 10.1109/JAS.2022.105515.

Xiao X, Fang Y. (2021). Motor imagery EEG signal recognition using deep convolution neural network. *Frontiers in Neuroscience*. 2021; 15:655599. <https://doi.org/10.3389/fnins.2021.655599>.

Yang L, Song Y, Ma K, Xie L. (2021). Motor imagery EEG decoding method based on a discriminative feature learning strategy. *IEEE Transactions on Neural Systems and Rehabilitation Engineering*. 2021; 29:368-79. DOI: 10.1109/TNSRE.2021.3051958.

Yu, X., Aziz, MZ, Sadiq, MT, Fan Z, Xiao G. (2021). A new framework for automatic detection of motor and mental imagery EEG signals for robust BCI systems. *IEEE Transactions on Instrumentation and Measurement*. 2021; 70:1006612. DOI: 10.1109/TIM.2021.3069026.

Zeng H, Xia N, Tao M, Pan D, Zheng H, Wang C, Xu F, Zakaria W, Dai G. (2023). DCAE: A dual

conditional autoencoder framework for the reconstruction from EEG into image. *Biomedical Signal Processing and Control*. 2023; 81:104440. <https://doi.org/10.1016/j.bspc.2022.104440>.

AUTHOR BIOGRAPHIES



Vishwesh Jayashekar is currently working as Associate Professor in the Department of Computer Science & Engineering at GSSS Institute of Engineering & Technology for Women, Mysore. He obtained Bachelor Degree in Computer Science & Engineering from PES College of Engineering, Mandya, Karnataka State, India in 2009. M. Tech from University of Mysore, Mysuru, Karnataka State, India in 2011. Ph D from VTU, Belagavi in 2023. He has 12 years of teaching experience. currently he published 4 international papers.



Raviraj Pandian completed his doctorate degree in Computer Science and Engineering in the area of Image Processing. He holds a position of Director-IQAC and Professor in the Department of Computer Science and Engineering at GSSS Institute of Engineering and Technology for Women, Mysore, Karnataka. He has 19 years of teaching and research experience. He has published more than 92 papers in international journals and conferences. At present he is guiding the Ph.D. research scholars in the areas of image processing, pervasive and cloud computing, and bio-inspired algorithms and robotics. He has received the project grant Rs.5 Lakhs from the VGST, Govt. of Karnataka for the “Underwater Robotic Fish for Surveillance and Pollution monitoring”. He has received the awards and recognitions such as ‘Rhastriya Gaurav Award-2015’, ‘Shri P.K. das Memorial Best Faculty Award-2012’, ‘Young Achiever Award-2016’. He can be contacted at email: raviraj@gsss.edu.in.



Rajashekar Mallajamma Basavarajgowda is currently working as Associate Professor in the Department of Computer Science & Engineering at GSSS Institute of Engineering & Technology for Women, Mysore. He obtained Bachelor Degree in Computer Science & Engineering from Coorg Institute of Technology, Ponnampet, Karnataka State, India in 2008. M. Tech from National Institute of Engineering, Mysore, Karnataka State, India. Ph D from VTU, Belagavi in 2023. He has 16 years of teaching experience. currently he published 6 international papers.